Simulation of Offshore Wind System with Three-Level Converters: HVDC Power Transmission in Cloud Scope

M. Seixas, R. Melício, V. Mendes, M. Collares-Pereira, M. Santos

Simulation of Offshore Wind System with Three-Level Converters: HVDC Power Transmission in Cloud Scope

M. Seixas[1,2,3], R. Melício[1,2], V.M.F. Mendes[2,3],
M. Collares-Pereira[2], M. P. dos Santos[2]

[1]IDMEC/LAETA, Instituto Superior Técnico, Universidade de Lisboa, Lisbon, Portugal
[2]Universidade de Évora, Évora, Portugal, ruimelicio@gmail.com
[3]Instituto Superior of Engenharia de Lisboa, Lisbon, Portugal

Abstract. This paper is on a simulation for offshore wind systems in deep water under cloud scope. The system is equipped with a permanent magnet synchronous generator and a full-power three-level converter, converting the electric energy at variable frequency in one at constant frequency. The control strategies for the three-level are based on proportional integral controllers. The electric energy is injected through a HVDC transmission submarine cable into the grid. The drive train is modeled by a three-mass model taking into account the resistant stiffness torque, structure and tower in the deep water due to the moving surface elevation. Conclusions are taken on the influence of the moving surface on the energy conversion.

Keywords: Offshore wind turbine, HVDC, three-level converter, simulation.

1 Introduction

Over the last decades, the energy primary sources like oil, coal, nuclear and natural gas have been used as the main source of energy for conversion into electric energy [1]. Nonetheless, disadvantageous circumstances are pointed out in the use of these sources, for instances: for fossil-fuel, the harmful on the environment and the cost subject to market instability and tending to increase in the long run. Forecasts for non-nuclear and non-renewable energy sources are in support of an envisaged scarcity pointing to the exhaustion on those sources in less than a century [2]. Exploitation on renewable energy sources have emerged by support of country polices or by more in-depth protocols such as the Kyoto Protocol as a response to harmful on the environment, instability and increasing fuel costs.

The wind energy source is the one within the exploitation of renewable energy sources that has experienced a greater development [3]. This development has achieved such a level that there is an increasing difficulty in new deployment, i.e., a difficulty to find new appropriate places for onshore wind farms. Particularly, a considerable exhaustion on convenient places is reported for Europe [4]. Thus, there is an interest in the exploitation of offshore wind energy, which has the benefits of available vast sea areas and of more favorable wind conditions, than those on land. Higher values of wind speed with less variation, because of the non existence of obstacles are encouraging offshore deployment [5]. Deployment of offshore wind

energy has a power transmission technology depending on the distance from the floating platform to onshore: for distances less than 60 km is proposed to use high-voltage ac (HVAC); for longer distances is proposed high voltage dc (HVDC) [6].

Deployment of offshore wind energy has a less concern with visual and noise impact, allowing the use of wind turbines with larger rotors, allowing a higher value for the installed power. The increase in size of the wind turbines implies particular design. As fact the blades are larger, more flexible and tend to bend. Therefore, the model for the drive train has to capture this fact and this paper proposes a three-mass (TM) model to take into account the concern with the dynamic of the blades, the structure and the moving floating platform.

2 Relationship to Cloud-based Solutions

The global growing demand for energy led to the deployment of new energy conversion called distributed energy located closely to the electric load to be served. A variety of small grid-connected devices referred to as distributed energy resources (DER) are introduced to allow the flow of distributed energy. DER systems typically use renewable energy sources, and increasingly play an important role for the electric grid. With the increasing demand for electricity and the growth of distributed generation (DG) there is a concern with the ability of the existing electric grid to accommodate the needed transformation. Thus, new insight into the electric grid is required and the concept of Smart Grid (SG) is on the way. SG conception includes the area of smart technologies able to quantify in real time the energy consumption, the power quality and ability to avoid or pre-detect eventual faults [7]. Vital for the SG conception is an architecture that guaranties safety and reliability. A layered processing system seems a good option, gathering information about the SG components delivering an insight into the behavior of the system, which allows operators or machines to take action accordingly, over a services platform. The designed software and hardware structure can be transferred to a cloud architecture system, benefiting of existing Internet Cloud Services, as in Fig. 1, to process the data storage and data transfer in real-time with cheap processing costs [7]. Due to safety issues, one expects that the best approach to the deployment of the cloud architecture in electrical grids will be a private cloud. Private clouds are projected and built exclusively for a single organization, which has full control over how applications and data are deployed in the cloud [8]. Every step in the project raises security issues that must be addressed to prevent vulnerability [9]. Due to the vulnerability, the SG approach advocates the use of a layered system that supports the integration of sensors and actuators, acting in a bidirectional data exchange, thus providing an introduction in the accelerating integration of SG services [10].

3 Modeling

The wind speed intermittence and variability stochastic character are possible to model by a deterministic sum of harmonics ranging 0.1–10 Hz as is indicated in [11] given by

$$u(t) = u_o[1 + \sum_k A_k \sin(\omega_k\ t)] \tag{1}$$

where u is the wind speed with perturbation, u_o is the average wind speed, A_k is the magnitude of the k eigenswing, ω_k is the eigenfrequency of the k eigenswing.

Offshore structures are influenced by marine wind and wave dynamics. The marine wave model [12] is given by

$$\eta(x, y, t) = \sum_{i=1}^{n} \eta_a(i) \cos[\vartheta(i)t + \varepsilon(i) - \phi(i)(x\cos(\psi(i)) + y\sin(\psi(i))] \tag{2}$$

where $\eta(x, y, t)$ is the wave elevation for (x, y) position as a function of time, η_a is the vector of harmonic wave, ϑ is the vector of harmonic wave frequencies, ε is the vector of harmonic wave phases (random), ϕ is the vector of harmonic wave numbers and ψ is the vector of harmonic wave directions.

The offshore wind system (OWS) apart from the wind turbine has a rectifier linking a permanent magnet synchronous generator (PMSG) to a first set of two capacity banks. A high voltage DC transmission submarine cable links the first set of two capacity banks to a second one connected to an inverter, injecting the energy into an electric grid through a second order filter. The OWS is shown in Fig. 1.

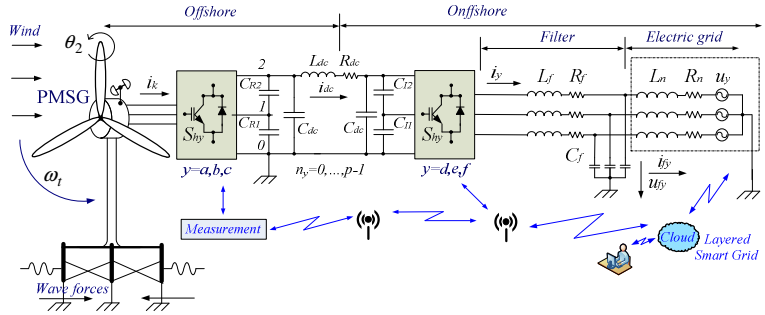

Fig. 1. Offshore wind system with three-level converter, HVDC.

The drive train is modeled by a three-mass model. The first mass concentrates the inertia of the flexible part of the blades; the second mass concentrates the rigid part of the blades, hub, tower and platform, discarding the movement between the different elements, but including the floating motion influence on the second mass; the third mass concentrates the inertia of the generator. The equations for modeling the motion of the drive train are based on the torsional version of the second law of Newton and are given by

$$\frac{d\omega_t}{dt} = \frac{1}{J_b}(T_t - T_{db} - T_{bs}) \tag{3}$$

$$\frac{d\omega_h}{dt} = \frac{1}{J_h}(T_{th} + T_{bs} + T_{sm} - T_{dh} - T_{hs}) \tag{4}$$

$$\frac{d\omega_g}{dt} = \frac{1}{J_g}(T_{hs} - T_{dg} - T_g) \tag{5}$$

where ω_t is the rotor angular speed at the flexible blades part, J_b is the moment of the inertia of the rotating parts at the flexible blades part, T_t is the mechanical torque, T_{db} is the resistant bearing torque due to the damping at the flexible blades part, T_{bs} is the resistant shaft stiffness torque between the flexible blades part and hub, ω_h is the rotor angular speed at the hub plus rigid blades part, J_h is the moment of the inertia of the rotating parts of hub plus the rigid blades part, T_{th} is the mechanical torque of the rigid blades part, T_{sm} is the tower and platform stiffness torque due to floating surface motion, T_{dh} is the hub bearing resistant torque, T_{hs} is the shaft stiffness torque between hub and generator, ω_g is the rotor angular speed at the generator, J_g is the moment of inertia of the rotating parts of the generator, T_{dg} is the generator bearing resistant torque, T_g is the electric torque.

The equations for the PMSG modeling can be retrieved in diverse texts [13]. In the PMSG to avoid demagnetization of permanent magnet a null reference stator direct component current $i_{sd}^{*} = 0$ is imposed [14]. The three-level converter has twenty-four unidirectional commanded insulated gate bipolar transistors (IGBTs) to implement the rectifier or the inverter functionality [15]. The group of four IGBTs associated in the same phase is said to be the converter's y leg. The switching variable n_y with $n_y \in \{0,1,2\}$ is used to identify the IGBT i state in the leg y of the three-level converter. The switching variable n_y is given by the switching function of the IGBT. The switching variable as shown in [15] is given by

$$n_y = \begin{cases} 2, & (S_{cy}\ e\ S_{dy}) = 1\ \ e\ \ (S_{ay}\ e\ S_{by}) = 0 \\ 1, & (S_{by}\ e\ S_{cy}) = 1\ \ e\ \ (S_{ay}\ e\ S_{dy}) = 0 \\ 0, & (S_{ay}\ e\ S_{by}) = 1\ \ e\ \ (S_{cy}\ e\ S_{dy}) = 0 \end{cases} \tag{6}$$

The level variable δ_{jny} with $j \in \{1,2\}$ used to establish the charging state of the capacitor banks [15] is given by

$$\delta_{jn_y} = \begin{cases} 0 & j > n_y \\ 1 & j \le n_y \end{cases} \tag{7}$$

The rectifier output voltage is given by

$$u_{sy} = \frac{1}{3}\sum_{j=1}^{2}(2\delta_{jn\,y} - \sum_{\substack{l=a \\ l\neq y}}^{c}\delta_{jnl})U_{CRj} \qquad y \in \{a,b,c\} \tag{8}$$

The DC voltage at the first set of capacity banks U_{dcRj} rectifier side is given by

$$\frac{dU_{dcR}}{dt} = \sum_{j=1}^{2}\frac{1}{C_{Rj} + C_{dc}} i_{CRj} \tag{9}$$

The linking between the first set of two capacity banks on offshore to a second one on onshore is assumed to be by a high voltage DC transmission submarine cable. The submarine cable is modeled by a π equivalent circuit [13]. The current i_{dc} in the cable is given by

$$\frac{di_{dc}}{dt} = \frac{1}{L_{dc}}(U_{dcR} - U_{dcI} - R_{dc} i_{dc}) \tag{10}$$

The DC voltage at the second set of capacity bank U_{dcI}, inverter side, is given by

$$\frac{dU_{dcI}}{dt} = \sum_{j=1}^{2}\frac{1}{C_{Ij} + C_{dc}} i_{CIj} \tag{11}$$

The electric grid is modeled by an equivalent three-phase active symmetrical circuit given by a series of a resistance and an inductance. Hence, the electric current injected, into the electric grid is given by

$$\frac{di_{fy}}{dt} = \frac{1}{L_n}(u_{fy} - R_n\, i_{fy} - u_y) \qquad y = \{d, e, f\} \tag{12}$$

This model is normally used in transient simulations and corresponds to what is said to be an infinite grid model linked by the equivalent series impedance.

4 Control Method

A classical PI controller is used to acquire the current references. IGBTs on/off switching states imply that the three-level converter is a time variant system. Therefore the sliding mode (SM) control strategy is crucial to alter the three-level converter, assuring the assortment of the proper space vectors. Additionally, PWM by space vector modulation (SVM) associated with SM is used for triggering the IGBTs. The SM strategy's aim is to let the system slide along a predefined dynamic, also

known as sliding surface $A(e_{\alpha\beta},t)$, by changing the system structure, i.e., by changing the IGBTs on/off state. The IGBTs can only switch at finite frequency, due to physical limitations causing the control current not to be able to follow exactly the reference current, thus creating an error $e_{\alpha\beta}$. Hence, to maintain the system within the neighboring of the sliding surface, the state trajectory must comply with the conditions [15] given by

$$A(e_{\alpha\beta},t)\ \ dA(e_{\alpha\beta},t)/dt < 0 \tag{13}$$

A small error is acceptable in practice and a convenient achievement of this strategy is accomplished with hysteresis comparators [15]. If the current error, given by the comparators hysteresis output $\sigma_{\alpha\beta}$ is quantified in five levels is possible to relate the space vectors with the current error. So $\sigma_{\alpha\beta}$ are integers numbers taking values in the set $\{-2,-1,0,1,2\}$. There are redundant vectors which correspond to different voltage level selection. The control strategy carries out a reduction on the capacitors banks unbalancing voltage by considering three vector tables [15], which take in account the voltage level of each capacitor bank by the defining the vector to be used. The output vectors for the level 0, level 1 and level 2 in the $\alpha\beta$ plane for the three-level converter are shown in Fig. 2.

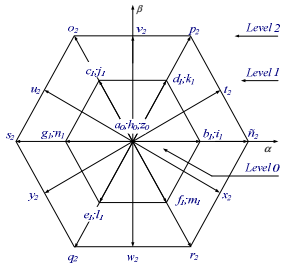

Fig. 2. Three-level inverter, output space vectors.

5 Case Study

The OWS has a nominal power of 2 MW. The capacity banks have a value of 65 mF. The filter have a R_f of 8 Ω a L_f of 500 μH and a C_f of 50 mF. The IGBTs switching frequency is 10 KHz. The mathematical model for the OWS with the three-level converter is implemented in Matlab/Simulink without the use of Power System Blockset. The wind speed considered has a profile defined by having an average speed starting with a value of 10 m/s followed by a ramp increase stabilizing after 1.5 s with an average speed of the 20 m/s, i.e., between 1.5 s and 4 s the wind average speed is constant. The significant wave height and the frequency are respectively 10 m and 0.25 Hz. The reference voltage and the DC voltages on the capacitor banks with the control strategy for selection of the vectors without unbalancing at the

rectifier side are shown in Fig. 3. The DC current at the submarine cable is shown in Fig. 4.

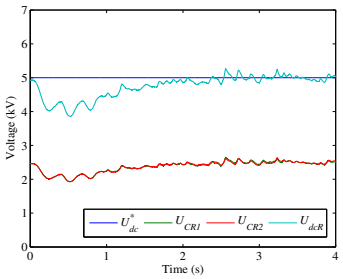

Fig. 3. DC voltages at the capacitor banks rectifier side.

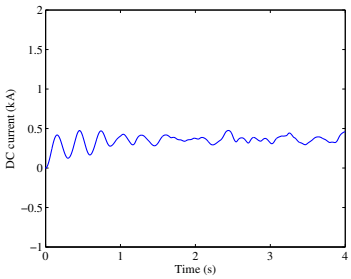

Fig. 4. DC current at the submarine cable.

The instantaneous current injected into the electric grid is shown in Fig. 5.

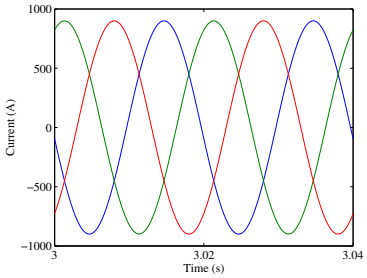

Fig. 5. Current injected into the electric grid.

The average THD for the current injected into the electric grid is 0.53%. Hence, the THD of the output current is lower than the 5% limit imposed by IEEE-519 standard.

6 Conclusions

Increased wind power penetration leads to new technical challenges, transient stability and power quality. In this paper, a model for a simulation study is presented for offshore wind system equipped with a PMSG with a back-to-back neutral point clamp three-level power converter with HVDC transmission. The case study presented is intended to evaluate the offshore wind system behavior, taking into account the wind and the marine wave perturbations. The simulation carried out is in favor that the perturbation due to the marine wave has a negligible effect on the system performance. This fact is due to two situations: first the wave frequency is smaller when compared to the frequency of the wind gust; and second the floating platform is stable. So, the system feels little mechanical vibrations due to the marine waves. The simulation study revealed a good performance of the proposed offshore wind system

with the three-level power converter and HVDC link. Although, there are effects on the current output of the power converter, the average value for the THD of the current injected into the electric grid is lower than 5% limit referred as to be imposed by IEEE-519 standard.

Acknowledgments. This work was partially supported by Fundação para a Ciência e a Tecnologia, through IDMEC under LAETA, Instituto Superior Técnico, Universidade de Lisboa, Portugal.

References

1. Tao, M., Hongxing, Y., Lin, L.: A feasibility study of a stand-alone hybrid solar–wind–battery system for a remote island. Applied Energy, 121, 149–158 (2014)
2. Ishugaha, T.F., Li, Y., Wang, R.Z., Kiplagat, J.K.:Advances in wind energy resource exploitation in urban environment: A review. Renewable and Sustainable Energy Reviews, 37, 613-626 (2014)
3. McKenna, R., Hollnaicher, S. , Fichtner, W.: Cost-potential curves for onshore wind energy: A high-resolution analysis for Germany. Applied Energy, 115, 103-115 (2014)
4. Soukissian, T.: Use of Multi-Parameter Distributions for Offshore Wind Speed Modeling: the Johnson S_B Distribution. Applied Energy 111, 982–1000 (2013)
5. Lange, B., Larsen, S., Højstrup, J., Barthelmie, R.: Importance of thermal effects and sea surface roughness for offshore wind resource assessment. Journal of Wind Engineering and Industrial Aerodynamics, 92, 959-988 (2004)
6. Gil, M.P., Gomis-Bellmunt, O., Sumper, A., Bergas-Jané, J.: Power generation efficiency analysis of offshore wind farms connected to a SLPC (single large power converter) operated with variable frequencies considering wake effects. Energy, 37, 455 468 (2012)
7. Ayodele, T.R., Jimoh, A.A., Munda, J.L, Agee, J.T. Challenges of Grid Integration of Wind Power on Power System Grid Integrity: a Review. International Journal of Renewable Energy Research, 2, pp. 618–626 (2012)
8. Mell, P., Grance, T.: The NIST Definition of Cloud Computing. Recommendations of the National Institute of Standards and Technology, NIST (2011)
9. Is a private cloud really more secure?, http://cloudandcompute.com/private-cloud/private-cloud-more-secure/
10. Batista, N.C., Melício, R., Mendes, V.M.F.: Layered Smart Grid Architecture Approach and Field Tests by ZigBee Technology. Energy Conversion and Manag., 79, 721–730 (2014)
11. Akhmatov, V., Knudsen, H., Nielsen, A.H.: Advanced Simulation of Windmills in the Electric Power Supply. Int. J. Electr. Power Energy Systems 22, 421–434 (2000)
12. Eikeland F.N.: Compensation of wave-induced motion for marine crane operations. MSc. Thesis, Norwegian University of Science,16–26 (2008)
13. Ong, C. –M.: Dynamic Simulation of Electric Machinery: using Matlab/Simulink, pp. 259–350. Prentice-Hall, New Jersey (1998)
14. Senjyu, T., Tamaki, S., Urasaki, N., Uezato, K.: Wind Velocity and Position Sensorless Operation for PMSG Wind Generator. In: 5th Int. Conf. on Power Electronics and Drive Systems, pp. 787–792 (2003)
15. Seixas, M., Melício, R., Mendes, V.M.F.: Fifth Harmonic and Sag Impact on PMSG Wind Turbines with a Balancing New Strategy for Capacitor Voltages. Energy Conversion and Management 79, 721–730 (2014)